



**Universiteit
Leiden**
The Netherlands

Development and application of cryo-EM tools to study the ultrastructure of microbes in changing environments

Depelteau, J.S.

Citation

Depelteau, J. S. (2022, January 12). *Development and application of cryo-EM tools to study the ultrastructure of microbes in changing environments*.

Retrieved from <https://hdl.handle.net/1887/3249707>

Version: Publisher's Version

License: [Licence agreement concerning inclusion of doctoral thesis in the Institutional Repository of the University of Leiden](#)

Downloaded from: <https://hdl.handle.net/1887/3249707>

Note: To cite this publication please use the final published version (if applicable).

CHAPTER 6

Advanced methods for processing of large volume samples for cryogenic electron tomography

Jamie S. Depelteau¹, Jeroen Mesman², Janine Liedtke¹, Katrina A. Gundlach¹, Ariane Briegel¹

¹ Department of Microbial Sciences, Institute of Biology Leiden, Leiden University, Sylviusweg 72, 2333 BE Leiden, The Netherlands

² Department of Fine Mechanics, Leiden University, The Netherlands

Abstract

To understand complex biological systems, we need to gain insight into individual cells in the context of multicellular systems. However, the structural details about how cells interact with each other in complex systems remains elusive, mainly due to their volume. Recently, techniques such as cryogenic electron tomography (cryo-ET) can be used to visualize individual cells at macromolecular scale. A variety of techniques have been developed for examining large volume samples, including high pressure freezing, freeze substitution, ultramicrotomy, and cryogenic focused ion beam scanning electron microscopy (cryo-FIB SEM). In combination, these techniques have provided the means to gain unique insights into multicellular structure, but their application are still not routine and they are affected by artifacts from sample preparation steps. Here, we set out to develop a new workflow based on new and already available methods to prepare large volume samples suitable for cryo-ET. We tested our workflow using variety of different samples, including animal and plant tissue as well as bacterial colonies. We found that conventional pulled glass needles were unsuitable for nanobiopsies, leading us to explore the 3D printing of acrylic needles. These needles allowed us to successfully obtain core samples from bacterial colonies on an agar plate and demonstrated the potential to obtain a sample from soft tissue. The isolated nanobiopsy samples were then high pressure frozen, recovered, and stored for trimming steps. In addition, we were able to freeze samples directly on grids, which were then further processed by ultramicrotomy and imaged using cryo-FIB SEM. Together we show that the acrylic needles offer a unique opportunity to collect a sample at the micrometer scale which is suitable for subsequent processing as preparation for cryo-ET.

Introduction

Understanding the complex biological world at the nanoscale is a challenging endeavor. A key component to achieving this goal is visualizing these processes within the cellular and multicellular context. In the past, many imaging techniques have been developed to examine individual cells and their contents. However, only a few of these methods can resolve details at a high resolution to visualize individual large proteins or protein complexes.

In the past years, cryogenic transmission electron microscopy (cryo-TEM) has become an essential tool to study biological samples in a near-native context with optimal structural preservation (2, 75). For cryo-TEM, thin samples such as small cells or isolated protein complexes can be used. The typical workflow of the cryo-TEM sample preparation consists of pipetting a sample onto an EM support grid, removal of the excess liquid by blotting with filter paper, and plunge freezing the sample into a liquid nitrogen cooled cryogen. This preparation step immobilizes the sample in non-crystalline, amorphous ice while preserving its delicate ultrastructure (1). Once inserted into the cryogenic electron microscope, the sample can be imaged. Subsequent computational methods are then used to reconstruct a 3D volume of the sample.

Two types of cryo-TEM are regularly used for imaging of biological samples: single particle analysis and cryogenic electron tomography (cryo-ET). Single particle analysis focuses on protein or protein complexes and relies on a homogeneous sample. However, for samples that are heterogeneous, such as entire small cells or tissues, the method of choice is cryo-ET. This technique requires tilting of the sample while collecting multiple images of the same target. The resulting set of images can then be used to generate a 3D volume of the target at macromolecular resolution. Both techniques are now routinely used to address a wide variety of biological questions, including protein complex structures and their conformational changes, to the structure and function of macromolecular machines in their cellular context (for example, the flagellar motor; the spike complex of SARS-CoV-2 ; and the F6 chemotaxis array)(79, 86, 125).

To truly understand how those molecular machines are used and function within an even more complex system like tissue, biofilms and others, detailed insight into the structural interactions between cells and tissues is necessary. To address such research questions, cryo-ET has also proven very powerful for exploring the inner depths of cells and tissues (84, 88, 126–128). However, imaging such highly complex samples to investigate interactions between cells and tissues poses many

challenges that have so far limited the application of cryo-ET. The goal of this work is to develop techniques and workflows that allow for the ultrastructural analysis of large volume samples (LVS) using cryo-ET. LVSs are defined as samples that cannot be processed through the well-established cryo-EM workflow outlined above.

Plunge freezing is limited to a sample thicknesses of approximately 5-10 μm depending on the type and contents of the sample (1). Widely used samples that reach this thickness limitation are eukaryotic cells that are directly grown on gold support grids. When the cell attaches and spreads across the grid, the outer regions of the cell are within the vitrification range of plunge freezing. However, the cell thickness increases around the nucleus of the cell. These thicker areas of the cell often cannot be properly vitrified. Instead, crystalline ice formation is common in these areas, and the result of this improper freezing compromises the ultrastructural information of the sample. Thus, any sample that exceeds the thickness limitation for vitrification by plunge freezing is defined as a LVS and requires an alternative preparation process (Fig. 1). In this case, samples are prepared primarily by high pressure freezing (HPF). HPF is able to fully vitrify samples up to a thickness of about 250 μm using high pressure, extreme cold, and short freezing protocols (5, 129).

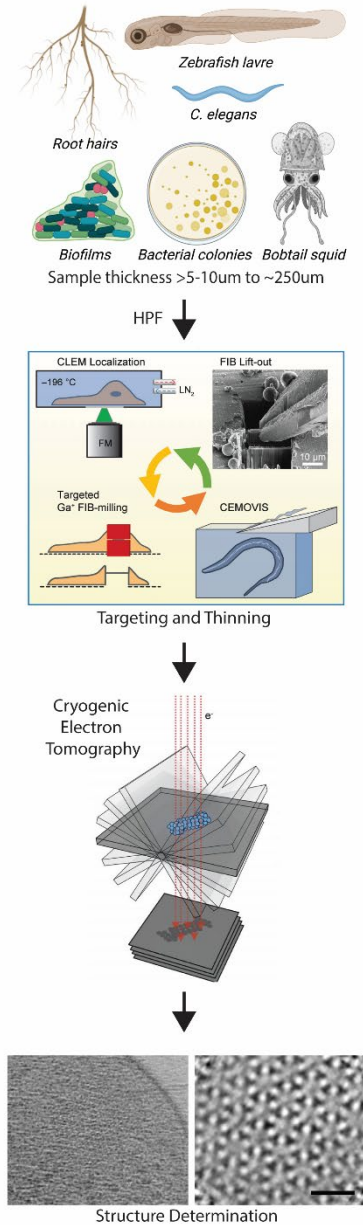


Figure 1. Overview of large volume workflow for cryogenic electron microscopy. Examples of large volume samples (created in Biorender.com). Once the sample is vitrified by high pressure freezing (HPF), additional sample thinning must occur. Traditionally this occurs using cryo-FIB SEM to either directly make lamella or in combination with a cryo-lift out device, or by direct thinning using CEMOVIS. These thinning methods can be targeted to areas of interest using CLEM. Once the target thickness of ~200 nm is achieved, the sample is transferred to the EM for image cryo-ET. The 3D volume is computation reconstructed, which can then be used for structure determination (left, top view of F6 chemotaxis array in a *Vibrio cholerae* cell; right, sub tomogram averaging of the top of F6 chemotaxis system revealing the hexagonal structure). Adapted from (2).

Despite the possibility to vitrify such large samples, they remain too thick for direct imaging with cryo-TEM. For instance, using the eukaryotic cell example noted above, as you approach the nucleus, the electron beam is unable to penetrate the sample, which produces a black image that is devoid of useful information. The general rule of thumb for suitable sample thickness is that two times the electron voltage is the maximal sample thickness (in nanometer) that can be effectively imaged with cryo-EM (130). For example, using a cryo-EM with an electron source operating at 300 keV, samples with a thickness of up to 600 nm are considered the upper limit that will result in interpretable data. However, in the case of cryo-electron tomography, the sample is tilted during data collection, which increases the thickness at higher tilt angles. In general, thinner samples lead to higher resolution data, and the optimal sample thickness for imaging is about 150-200nm. Thus, cryo-EM is still significantly limited by the types of samples that can be imaged. To make this imaging method accessible for LVSs, the samples need to be both properly vitrified and subsequently thinned to a thickness that is compatible for the commercially available cryo-electron microscopes (Fig. 1).

One established method for the thinning of thick cryo-TEM samples is to thinly section the frozen sample using glass or diamond knives in a cryo-ultramicrotome. This procedure is similar to preparing plastic sections for traditional EM. However, in the case of the cryo-TEM sample, the ultramicrotome has a cryo-chamber attached, and specialized knives are used for trimming and producing sections of 70-300 nm at cryogenic temperatures. This technique is called cryogenic electron microscopy of vitreous sections, or CEMOVIS (Fig. 1) (6, 7, 131–133). CEMOVIS has been used successfully for the last twenty years, though it is known to require specialized training to do it well. Additionally, the sectioning process cause a number of known artifacts, such as compression and tears in the sections (134). The challenges and artifacts caused by CEMOVIS have limited its application for cryo-ET to a few specialized research groups. Nevertheless, it remains a valuable technique for thinning of LVS.

In recent years, advances in cryogenic focused ion beam (FIB) scanning electron microscopy (SEM) (cryo-FIB SEM) have made this method increasingly popular to process LVSs. With this technique, the SEM beam is used for targeting and monitoring of the vitrified sample, and an ion beam is used to remove enough material to allow imaging in the cryo-TEM (Fig. 1). The target thickness of these lamella is roughly 200 nm, though thinner is possible and may be advantageous depending on the biological questions. Currently this process is most often applied to eukaryotic cells that have been grown on a grid. But cryo-FIB SEM has also been used for the processing of even thicker samples such as biofilms and even an intact

C. elegans worm (84, 88, 135). Despite its proven potential for answering crucial biological questions, this technique can be daunting and time consuming. It requires many transfer steps that can introduce contamination to the sample, and it can take seven to eight hours to generate a limited number of lamella. Furthermore, the starting sample thickness before milling is limited to 20 μm or less. Thus, for samples of greater size, additional thinning steps are required before it is possible to mill with a cryo-FIB SEM and subsequent imaging with cryo-TEM.

Here we set out to develop novel LVS preparation methods for cryo-EM imaging. Building on established methods, we developed a biopsy needle designed to collect samples directly from the organism of interest. The sample-filled needle is then subjected to HPF, and ready for subsequent trimming either a cryo-ultramicrotome or cryo-FIB SEM, or both. The resulting thinned samples are destined for the cryo-TEM. After several iterations, we successfully collected core samples of *Streptomyces coelicolor* grown on solid media. This study provides evidence that biopsies at the microscale are obtainable, and with continued experimentation, this technique could open a new avenue for LVS processing and imaging by cryo-ET. Ultimately this technique will provide a new route to visualizing the multicellular complexes with unprecedented resolution.

Methods and materials

Biological specimens

Streptomyces coelicolor M145 was grown on minimal media supplemented with 1% mannitol and 1% glycerol as a carbon source. Production of the dark brown color was due to a pigmented antibiotic, actinorhodin, which its concentration was increased by adding 0.1% methyl jasmonate.

Zebrafish (*Danio rerio*) larvae used in these experiments were obtained by mating wild-type AB/TL adults according to established protocols (zfin.org), with the approval of the local animal welfare committee (DEC) of Leiden University (License # 10612), and in accordance with the EU Animal Protective Directive 2010/63/EU. All larvae were 4 or 5 days post fertilization and before the feeding stage and thus exempt for the EU Animal Protective Directive 2010/63/EU. Eggs were collected immediately after mating and were maintained at 28°C in artificial fresh water (60 mg/L Instant Ocean) until use.

Radishes were obtained from the local market within a few days of processing. The tips of the main root were used for sample testing.

Glass needles

Two types of glass needles were tested for use in obtaining samples. In our initial attempt we used borosilicate glass capillary tubes that are routinely used to create microinjection needles. In this case we used borosilicate glass capillaries GC100F-10; 1.0 mm outer diameter, 0.58 mm inner diameter (Harvard Apparatus, Kent, United Kingdom). The tubes were loaded onto a Flaming/Brown Micropipette Puller (Model P-97, Sutter Instrument Co., USA) with settings of heat = 50, EL = 40, and time = 15. These settings reliably produced needles with an outer diameter of approximately 200 μm and an inner diameter of 180 μm . Two needles were produced from each event. Subsequently, the tips were trimmed using a scalpel or fine tweezers (Fig. 2A). The resulting needles were then used on two types of material: 1.2% agarose plates and zebrafish larvae in two different sites: tail or gut.

The second type of needle did not require pulling to achieve desired inner diameters. In this case, BGCT 0.1 borosilicate capillary tubes were purchased (Capillary Tube Supplies Ltd., Cornwall, United Kingdom). These needles had an outer diameter of 0.1mm and wall thickness of 0.01mm. In this case we developed attachments that allowed for easy handling and targeting of the needles (Fig. 2B-E). The glass needle is attached to a handle (Fig. 3C), which could then be used to manipulate the needle during the polishing step (Fig. 2D) and the sample targeting and collection step (Fig. 2E). Once the needles were polished to sharpen the tip, they were tested on agar plates of various concentrations.

3D printed needles

As an alternative to glass needles, we decided to 3D print needles to our desired specification to gain increased precision and reproducibility. The needles were 3D printed using the Nanoscribe Photonic Professional GT 3D printer (Nanoscribe GmbH & Co. KG, Karlsruhe, Germany) and photo activatable resin. The needle design went through several iterations, each being tested using agar plates of various concentrations. Once an ideal design was identified, additional needles were printed and tested on various biological samples. Success was defined as the ability to retrieve a core sample from the material, with little visual evidence of significant distortions.

For the final testing of the needle design, the 3D printed needles were glued to a 200 μl pipette tip containing a pin (Fig. 4D, S1B). The pipette tip was then attached to a spring loaded injection device (Fig. S1A, S1B), which was mounted to a movable, mechanical arm that was magnetically anchored to the table. The needle was positioned approximately perpendicularly to the agar pad containing sample. Using a dissecting scope, the sample was aligned with the needle, and then the needle

was injected approximately 3mm into the sample. The agar plate was then moved away from the needle and the needle was transferred to the HPF for the freezing protocol.

High pressure freezing

Sample isolation was immediately followed by HPF using the Leica EM ICE (Leica Microsystems GmbH, Austria). Sample-containing needles were separated from its base at the tripartite junction (arrow, Fig. 2, S1C) and then loaded into the 200 μm deep side of a 3 mm 'type A' copper carrier prefilled with 1-hexadecene. An additional drop of 1-hexadecene was added to the μm deep side of a second 'type A' carrier and then combined with the sample containing carrier (the resulting total height inside the carrier was 300 μm). The carrier was then inserted into the carrier holder and automatically processed through the ICE. In some cases, a grid was inserted in between the sample and top carrier in an effort to freeze the sample directly to the grid. Frozen samples were retrieved and stored in a grid box liquid nitrogen until further processing (Fig. S1D).

For samples obtained without the needle, the samples were trimmed with a scalpel, inserted into the 200 μm deep side of a 3 mm 'type A' carrier, filled with 10% Ficoll, topped with a Quantifoil R2/2, 200 mesh copper grid, followed by the flat side of a 'type B' 3 mm carrier. For the plant root, the root sample was directly frozen with the Leica EM ICE using a similar set as the needle. For the zebrafish larvae, the sample was high pressure frozen with a Baltec HPM010.

Sample thinning

Frozen samples were removed from the carriers under liquid nitrogen or in liquid nitrogen vapor. Samples were either frozen directly on grids or mounted to a grid prior to thinning using a cryo-glue (3:2, 2-propanol:100% ethanol). Initial thinning occurred using the Leica EM UC7 mounted with the Leica EM FC7 cryo-chamber and equipped with an EM Crion antistatic device (Leica Microsystems). Trimming of the samples occurred at -160°C using a cryo-Trim 45 knife (Diatome). Fine sectioning occurred using the cryo-immuno diamond knife (Diatome). Trimmed samples were transferred to the Aquilos cryo-FIB SEM (Thermo Fisher Scientific (TFS), Waltham, MA, USA). The cryo-FIB SEM provided a general impression of the trimming quality and suitability for subsequent milling with the FIB.

Results

Zebrafish larvae processed through the traditional workflow

Our initial test of LSV preparation was done by directly freezing and milling of 5 dpf zebrafish larvae. Here, the tail and head were trimmed immediately prior to HPF so that it fit into the carrier, and an EM support grid was placed between the sample and the flat side of the carrier. After high pressure freezing, the sample naturally dislodged from the carrier sandwich and remained attached to the grid (Fig. 2). The sample-containing grid was clipped and evaluated using the Aquilos cryo-FIB SEM. The larva was found to be attached the grid (Fig. 2A-B). Rough milling was performed (blue circle in Fig. 2A), however, after several hours it became clear the sample would require extensive milling over several days using Aquilos to be suitable for cryo-ET (Fig. 2C, blue asterisk). After storage of the sample, we found the tissue had dislodged when the sample was loaded again into the Aquilos (Fig. 2D), ending the milling attempt. Based on this experience, we decided to explore additional options for thinning of the sample before and after it was frozen, leading us to the testing of a biopsy needle.

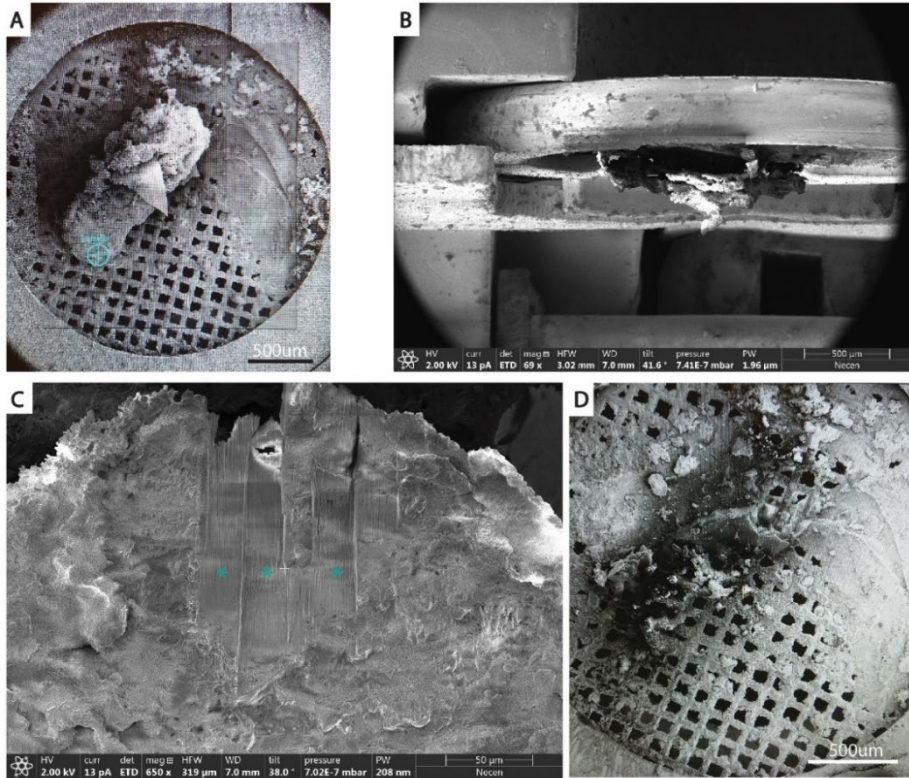


Figure 2. Overview of milling attempt of 5dpf zebrafish larvae. The trimmed zebrafish larva was trimmed and high pressure frozen directly on a grid. Upon visualization with the cryo-FIB SEM, the tissue appeared attached to the grid (A & B). FIB milling was attempted (A, blue circle is site of milling; C, blue asterisks) on the site noted in A and magnified in C. Following milling the sample was stored until the next milling session, which demonstrated a lack of tissue on the grid (D).

Glass needles

We next attempted sample extraction utilizing glass needles that had been pulled to specific inner diameter of approximately 100-200 μm . The needles proved to be too fragile and tips were too jagged and brittle to obtain an intact sample (Fig. 3A). In addition, during sample extraction it became clear that the needles were insufficiently sharp to puncture tissue with precision, especially in places where the sample was soft and pliable.

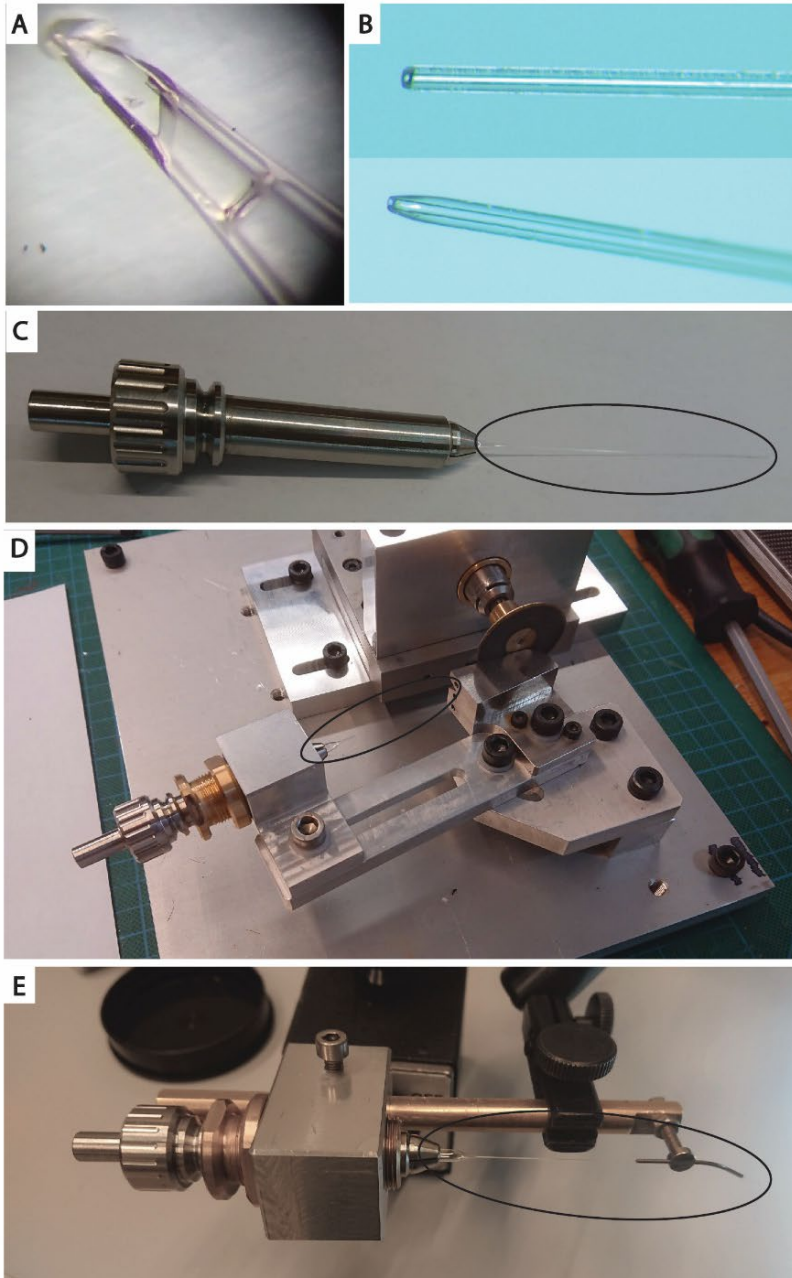


Figure 3. Example of glass needles and tools used to manipulate the needle. A. A representative image of a pulled glass needle following an attempt to extract a sample from an agar plate. B. Alternative needle design that required polishing of the edge rather than pulling of the needle. Due to the size and flexibility of the needle (black oval), tools were created to help with the handling (C), polishing (D), and targeting (E).

In an effort to increase consistency between the needles, we purchased glass capillary tubes with a specific inner and outer diameter, and then polished the tips to form a sharp point (Fig. 3B, top: unpolished, bottom: polished). In addition, we developed several tools used for handling of these needles, which improved our ability to move the needles between processing stages and sample extraction (Fig. 3C-E). In this case, we only tested the needles on agar plates of various concentrations. The needles continued to be too blunt and too flexible for suitable sample extraction, thus we explored alternative methods for needle production.

3D printed needles

After several unsuccessful attempts with the glass needles, we next explored the option of 3D printing needles to exact specifications. Most commercially available 3D printers do not have the ability to print accurately at the micron scale. Therefore, we used a specialized instrument that was available through our fine-mechanics department and that is capable to 3D print such items. In our case, we utilized the Nanoscribe Photonic Professional 3D printer, which uses two-photon technology to polymerize resin in a specific pattern. We designed and printed several versions of needles, keeping in mind the need for a sharp end that could help with the targeting and the incision. A common design feature included a three-prong tip with a thickness of 20 μm that was used for targeting of the needle at the site of injection. The needle was 1.65 mm in length with an inner diameter of 140 μm (size varied depending on the iteration but remained close to this diameter). An important component of the needle was the tripartite slits at the base of the needle (Fig. 4B arrow). These allowed any air pressure build up release when the sample enters the needle and prevents the sample from slipping out during retraction. The slits also provided a break point for the needle: once the sample was in the needle, it could be broken off and directly transferred to the sample carrier for subsequent high pressure freezing. Initial testing of this design achieved a core from 1.2% agarose plate (Fig. 4C, blue arrow highlighting the end of the sample). We next attempted to sample from a *Streptomyces coelicolor* colony, proved successful (Fig. 4D, arrow).

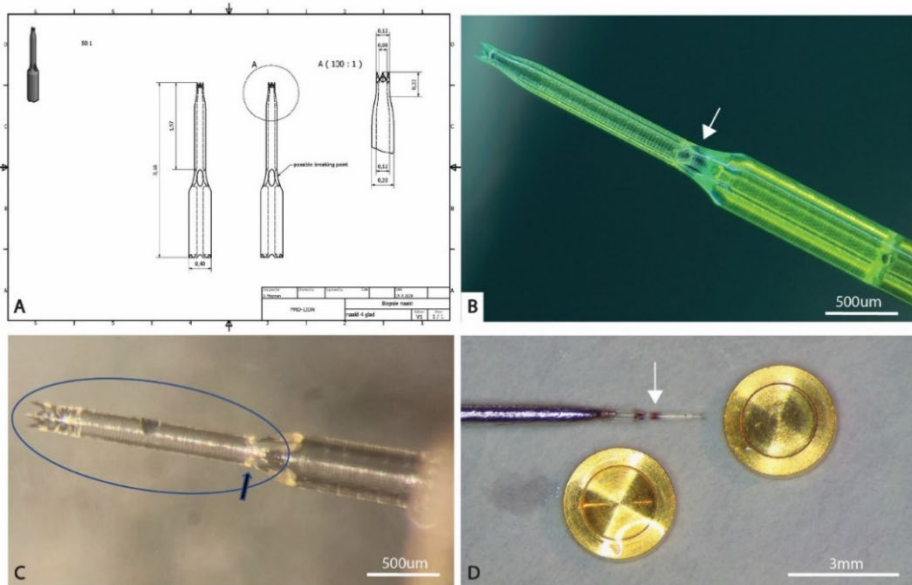


Figure 4. Overview of needle design and testing. A. Representative design of a 3D printed needle. B. Actual printed needle. The green color is due to autofluorescence of the resin. C. Proof of principle demonstrating the ability of the needle used to obtain a core from an agar plate. D. A mounted needle was used to obtain a core of a *Streptomyces coelicolor* colony from an agar plate. For reference, the two 3 mm carriers that will be used for HPF at located beside the sample filled needle.

High pressure freezing of sample filled needles

Prior to loading the sample-filled needle, the carrier is filled with a cryoprotectant to support the formation of vitrified ice. We tried various combinations of carriers and settled on the following assembly as the most optimal for the high-pressure freezing step: We placed the filled needle into a 200 μm deep side of a 'type A' carrier and sandwiched it with another cryoprotectant-filled 100 μm deep 'type A' carrier (Fig. 4D). The sandwich is then inserted into the high-pressure freezer, triggering the freezing process. We also tested a range of typically used cryoprotectants, such as 10% and 30% Ficoll and 1-hexadecene. 1-Hexadecene proved to be the most ideal cryoprotectant for our setup as it allowed for reasonable removal of the needle from the carrier without significant force. In addition to the cryoprotectant, we also coated our carriers in 1% soy lecithin dissolved in chloroform, which has been shown to ease the separation of the carrier sandwich and in releasing the sample from the carrier cavity. Once the frozen needle was removed, it was stored in a grid box until further processing.

Mounting and thinning of the sample

Following HPF, our intention was to directly mount the recovered needles to a cryo-EM support grid. This was done using the FC7 cryo-chamber of the ultramicrotome, cooled to -160°C . The grid box containing needles were transferred to the cooled chamber and allowed to acclimate while a grid was attached to the manipulator. When ready, the grid was placed in the chamber, cryo-glue (100% ethane: 2-Propanol in a 2:3 ratio) was dabbed onto the grid, and the needle was immediately transferred to the grid and attached to the glue. However, this process proved more challenging than expected. The needles themselves were frequently dropped in the chamber and unrecoverable. In addition, we found that the cryo-glue solidified too quickly, preventing the needle from attaching properly to the grid.

For samples that were frozen directly onto a grid, the grid had to be mounted before sectioning could begin. One sample, the radish root tip, made it to this step in the process (Fig. 5A). A 'type B' carrier was mounted to the chuck, with the 300 μm deep side facing the user. Cryo-glue was applied to the edges of the carrier and then the grid was quickly attached with a little pressure to create the bond (Fig. 5B). At this point the sample was allowed to equilibrate for several minutes before sectioning began. We successfully trimmed the sample using the cryo-Trim 45 diamond knife (note the reflective flat surface in Fig. 5B). Once trimming was complete, a cooled scalpel blade was used to detach the grid from the carrier, and transferred to a grid box for further processing in the cryo-FIB SEM. Imaging with the cryo-FIB SEM demonstrated that it was possible to successfully transfer the grid from the cryo-ultramicrotome, and that the sample was successfully trimmed and appeared structurally sound (Fig. 5C).

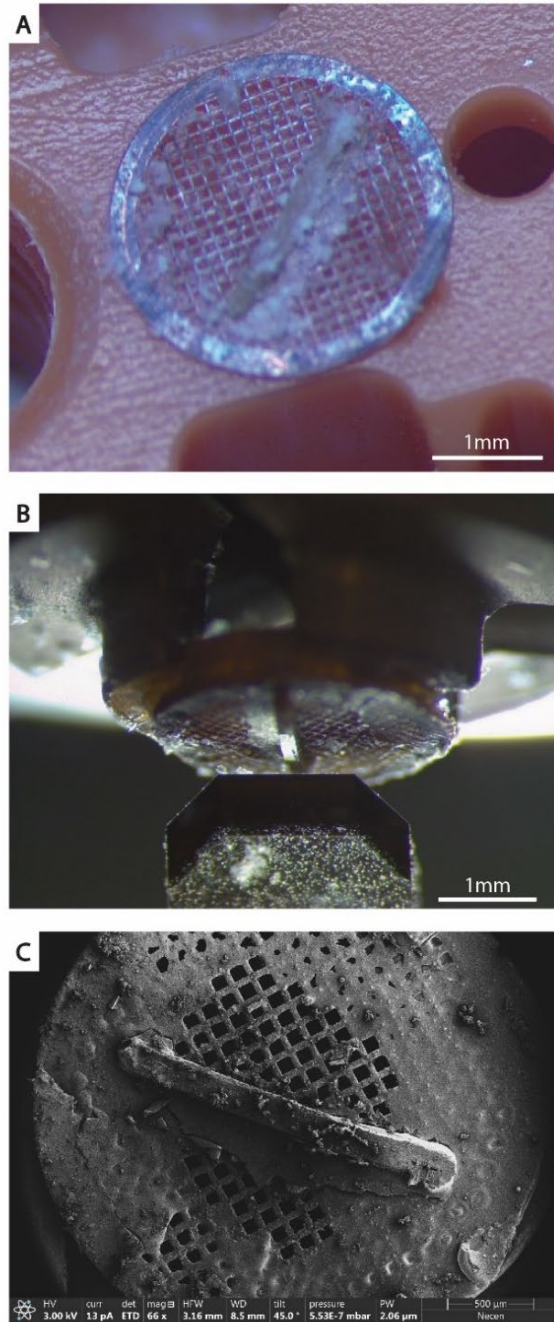


Figure 5. A radish root tip was isolated and HPF frozen directly on a grid (A). The sample-containing grid was then transferred to the cryo-ultramicrotome for sample thinning using a diamond knife (B). The sample was then transferred to the cryo-FIB SEM for inspection of sample quality following cutting.

Discussion

In this study we demonstrate the first few steps of a proposed LVS pipeline that is designed to prepare multicellular samples for cryo-ET. Our first attempts of sample recovery with glass needles were unsuccessful, demonstrating that a lack of a sharp edge and extreme flexibility were limiting factors. We could overcome these issues by using 3D printed needles. These needles could then be successfully used for sample collection and high pressure freezing of the sample. Using the 3D printed needle, we were successful in obtaining a core sample from a bacterial colony of *S. coelicolor*. When further analyzed, this type of sample could provide significant structural details about the aerial hyphae layer as well as the transition into the substrate. However, it remains to be demonstrated that the sample-filled needles can be taken through the remaining steps of the proposed workflow: sample thinning with the cryo-ultramicrotome and the cryo-FIB SEM, and ultimately imaging with the cryo-EM.

We were also able to directly freeze a sample on a grid using high pressure freezing. This protocol was successfully applied using a radish root tip: upon collection of the sample, the root tip was frozen directly on the grid, and subsequently trimmed using cryo-ultramicrotomy. This is an important step because it eliminates the need to mount the frozen sample to the grid before trimming. For the 3D printed needles, this processing step has proved challenging for us due to the size of the needle and the glue used to attach the needle to the grid. However, we believe additional practice in handling and transfer will allow this step to succeed. The root tip sample also demonstrated that following trimming, the sample can be successfully transferred to the cryo-FIB SEM for imaging and trimming. Again, this proof on concept supports our intended workflow. It is important to note that we have not completely processed a sample through the entire workflow. Instead, we have been able to successfully complete individual steps, which when combined with the right sample, we believe will prove to be a valuable tool for routine LVS processing.

Despite the challenges of LVS preparation, we see our workflow as the next step in the evolution of sample processing for cryo-ET. We combine several different methods, that are usually intended to be used individually or for different techniques, into a single workflow. As a way to make the LVS more manageable, we designed and implemented a 3D printed needle for obtaining biopsies from different samples. Up to this point, we have twelve versions of the needle that have been, or are being tested in different types of samples. We believe that with some trial and error, and intentional design, we will be able to apply the biopsy needle to

multiple sample types. The idea to use biopsy needles for sample collection is not a new one, as it is regularly used in the medical diagnostics. In addition, several successful attempts of creating a needle for sample preparation for EM were previously published (136, 137) that demonstrate that it is possible. Our study benefits from technological improvements, especially with 3D printing, which allows us to quickly redesign and implement changes that could be tissue specific. In addition, we have not reached the limits of the 3D printer, thus if we can get the current designs to work, we can reduce the size of the inner diameter of the needle which in turn reduces the amount of trimming necessary and would therefore ease the workflow.

The ultimate goal of this project is to better understand how bacteria interact with their host. Using the techniques developed here, we aim to structurally examine three different model systems: *V. cholerae* infected zebrafish larvae, endophytic bacteria found in plate roots, and the symbiotic relationship of *V. fischeri* with the Hawaiian bobtail squid (58, 138, 139). Each of these provides a unique opportunity to better understand how the bacteria's morphology and molecular machines impact their ability to interact with their respective hosts. For example, when *V. cholerae* colonizes a host, it uses a number of molecular machines in this effort: the F6 chemotaxis array to sense its environment, the flagella to move towards its desired niche, and the mannose-sensitive hemagglutinin (MSHA) pili for attachment to the epithelial cell surface (58). Using our LVS workflow, we could then use a natural host model of *V. cholerae* infection, the laboratory zebrafish, to better understand these steps in colonization and dissemination back into the environment (66). This model is especially interesting because other unknown factors might play a role in colonization. Being able to visualize the bacteria:epithelial cell interaction could provide new details about molecular machines that are involved in this process.

The next big advancements in cryo-ET lie in large volume sample processing. In the past several years, different commercial tools have been developed, such as the cryo-FIB SEM and the cryo-lift out device, which are beginning to allow researchers to shed light on complex, multicellular systems. However, opportunities for new technology such as our biopsy needles still exist. With this research we provide proof of principle that using micrometer length needles is a unique tool for obtaining cryo-ET suitable samples from LVS.

Acknowledgements

We are grateful for the assistance of Jan de Weert and Frederic Leroux for their training and assistance throughout the freezing and trimming workflow. We are also grateful to Carmen Lopez Inglesias and prof. dr. Peter Peters of the Maastricht Multimodal Molecular Imaging institute, M4i at Maastricht University for their assistance in our initial attempts to freeze the zebrafish larvae directly on a grid.

Supplementary Material

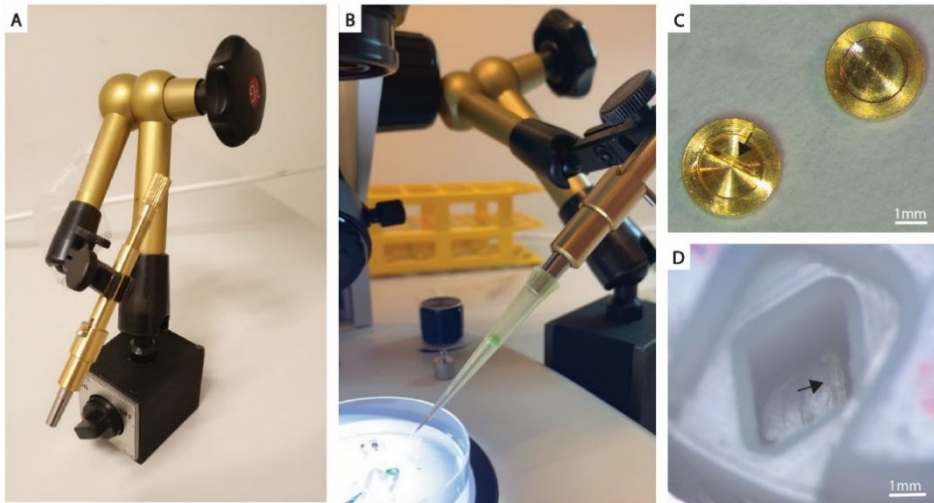


Figure S1. Overview of the sample acquisition process. A spring-loaded injector was attached to a mechanical arm (A) and the pipette tip with a needle was attached to the injector (B). Following sample retrieval, the needle was separation from the pipette tip, loaded into the 200 μm cavity of a 3 mm type A carrier containing 1-hexadecene (C, black arrow), and a second carrier was placed on top to form a sandwich. The sandwich is then high pressure frozen, the sample filled needle is recovered under liquid nitrogen in a grid box until further processing (D, black arrow).